

Indene Formation under Single-Collision Conditions from the Reaction of Phenyl Radicals with Allene and Methylacetylene—A Crossed Molecular Beam and Ab Initio Study

Dr Dorian S. N. Parker,^[a] Dr Fangtong Zhang,^[a] Dr Ralf I. Kaiser,*^[a]
Dr Vadim V. Kislov,^[b] and Dr Alexander M. Mebel*^[b]

Abstract: Polycyclic aromatic hydrocarbons (PAHs) are regarded as key intermediates in the molecular growth process that forms soot from incomplete fossil fuel combustion. Although heavily researched, the reaction mechanisms for PAH formation have only been investigated through bulk experiments; therefore, current models remain conjectural. We report the first observation

of a directed synthesis of a PAH under single-collision conditions. By using a crossed-molecular-beam apparatus, phenyl radicals react with C₃H₄ isomers, methylacetylene and allene, to

Keywords: combustion • gas-phase reactions • hydrocarbons • indene • molecular dynamics

form indene at collision energies of 45 kJ mol⁻¹. The reaction dynamics supported by theoretical calculations show that both isomers decay through the same collision complex, are indirect, have long lifetimes, and form indene in high yields. Through the use of deuterium-substituted reactants, we were able to identify the reaction pathway to indene.

Introduction

Soot from fossil fuel combustion is widely accepted as causing detrimental effects to health and the environment, such as being carcinogenic and mutagenic, as well as contributing to global warming.^[1–3] Soot is thought to be formed in a stepwise molecular-weight growth process, leading from small hydrocarbons and their C₂, C₃, and C₄ radicals, such as ethynyl (C₂H)^[4] and propargyl (C₃H₃)^[5] to aromatic molecules, such as benzene (C₆H₆) and the phenyl radical (C₆H₅), followed by the formation of polycyclic aromatic hydrocarbons (PAHs) and eventually particulate matter

(soot).^[6–9] The first step, the formation of the first aromatic ring structure (benzene and/or the phenyl radical), has been proposed through self-reaction of the propargyl radical,^[7,9–18] and more recently via the reactions of dicarbon (C₂)^[19] and ethynyl radicals (C₂H)^[4] with 1,3-butadiene (C₄H₆). The second step—the formation of a PAH—is anticipated to predominantly proceed through the reaction of benzene and/or phenyl radicals with unsaturated C₃ and/or C₄ hydrocarbons or their corresponding radicals.^[6,20] However, although the formation of PAHs through the reaction of phenyl radicals with C₃ and/or C₄ hydrocarbons has been proposed as a common route, no experimental evidence has been provided, to date, in which an individual PAH molecule has been formed in the gas phase as the result of a single collision event (crossed-molecular-beam experiments).^[21,22]

During recent decades, sophisticated flame tests have been the most popular investigatory technique designed to model conditions in internal combustion engines.^[23–33] These studies utilize mass spectrometry and gas chromatography or photoionization to determine the nature of the species in laminar premixed low-pressure flames consisting of the hydrocarbon fuel mixed with oxygen and argon.^[23–33] Chemical kinetic models of these flame results are exploited to suggest reaction mechanisms for how PAHs, and ultimately soot, might be formed. These models, however, rely on experimental thermodynamic data, rate constants, and most

[a] D. D. S. N. Parker, D. F. Zhang, D. R. I. Kaiser
Department of Chemistry
University of Hawaii at Manoa
Honolulu, Hawaii (USA)
Fax: (+1) 808-956-5908
E-mail: ralfk@hawaii.edu

[b] D. V. V. Kislov, D. A. M. Mebel
Department of Chemistry and Biochemistry
Florida International University
Miami, Florida (USA)
E-mail: mebela@fiu.edu

Supporting information for this article is available on the WWW under <http://dx.doi.org/10.1002/asia.201100535>.

importantly reaction products, which are not readily available and often educationally estimated. Therefore, reaction mechanisms for the formation of individual PAH molecules have been mainly conjectural. Among the PAHs, indene (C_9H_8) and naphthalene ($C_{10}H_8$) represent prototypes of C9 and C10 PAHs; these PAHs have been identified in sooting flames of the nonaromatic hydrocarbon-based fuels methane (CH_4),^[24] ethane (C_2H_6),^[23] acetylene (C_2H_2),^[27] propene (C_3H_6),^[29] *n*-butane (C_4H_{10}),^[30] and 1,3-butadiene (C_4H_6),^[31] as well as in aromatic fuels such as benzene (C_6H_6),^[28,32] toluene (C_7H_8),^[26,28,33] styrene (C_8H_8),^[28] ethylbenzene (C_8H_{10}),^[25,28] *ortho*-, *meta*-, and *para*-xylene (C_8H_{10}),^[28] cyclopentadiene (C_5H_6),^[34] and cyclopentene (C_5H_8).^[35] Herein, indene is proposed as a stepping stone toward complex PAHs.^[34,36]

But what experiment is advisable to study the formation of the indene molecule under single-collision conditions, that is, under the absence of any wall effects and consecutive reactions of the nascent reaction products? Considering the driving force for reactions of hydrocarbon radicals with closed-shell hydrocarbons, the reactions of the aromatic phenyl radical (C_6H_5) with methylacetylene (CH_3CCH) and allene (H_2CCCH_2) accesses the C_9H_9 potential energy surface, hydrogen loss from various reaction intermediates might lead to distinct C_9H_8 isomers, among them the aromatic indene molecule. What is known so far about the reactions of phenyl radicals with methylacetylene and allene from the literature? In 2002, Lindstedt and Rizos^[37] proposed a chemical kinetic model based on cyclopentene flame experiments conducted by Lamprecht et al.^[35] Indene formation was suggested through five routes: naphthalene oxidation ($C_{10}H_8+O_2 \rightarrow C_9H_8+CO_2$), allene addition to phenyl ($C_6H_5+C_3H_4 \rightarrow C_9H_8+H$), propargyl addition to a phenyl radical followed by stabilization of the reaction intermediate by a third body ($C_6H_5+C_3H_3 \rightarrow C_9H_8$), and acetylene addition to benzyl and methylphenyl radicals ($C_7H_7+C_2H_2 \rightarrow C_9H_8+H$). Allene addition to phenyl was proposed to be an important indene-formation pathway in this model. In 2006 Wang et al.^[38] exploited electronic structure methods to rationalize reaction mechanisms for indene formation from the pyrolysis of cyclopentadienyl, as conducted by Mulholland and co-workers.^[34] Wang et al. surmised that at low temperatures intramolecular addition pathways dominated, resulting in indene formation being greater than naphthalene and benzene formation; this was in accordance with experimental observations. They found that the two pathways with the lowest initial energy barriers resulted in indene formation through loss of a methyl group. In 1998 Marinov et al. conducted flame tests with *n*-butane and detected indene and the indenyl radicals.^[30] They surmised that the reaction mechanism was acetylene addition to benzyl ($C_6H_5CH_2$), yielding indene through hydrogen elimination. In 2001, Meyer et al.^[39] summarized early work completed by Bittner^[40] on PAH formation and proposed that allene addition to the phenyl radical was an important route to indene. The rate-determining step was suggested to be allene addition to the phenyl radical with a rate constant of

about $10^{13} \text{ cm}^3 \text{ mol}^{-1} \text{ s}^{-1}$ at 1000 K followed by multiple isomerization and hydrogen loss to yield indene. Bittner also identified that this atomic hydrogen elimination competed with the formation of stable monocyclic species, such as phenylallene ($C_6H_5CHCCH_2$).^[40] The reactions of phenyl radicals with allene and methylacetylene have also been studied using cavity ring-down spectroscopy by Lin et al.,^[41,42] who found absolute rate constants of $k_{\text{propyne}}(301\text{--}428 \text{ K}) = (3.68 \pm 0.92) \times 10^{11} \exp[-(1685 \pm 80)/T] \text{ cm}^3 \text{ mol}^{-1} \text{ s}^{-1}$ and $k_{\text{allene}}(301\text{--}421 \text{ K}) = (4.07 \pm 0.38) \times 10^{11} \exp[-(1865 \pm 85)/T] \text{ cm}^3 \text{ mol}^{-1} \text{ s}^{-1}$.

In addition to these studies, the reactions of a phenyl radical with allene and methylacetylene were also studied under single-collision conditions at high collision energies of up to 161 kJ mol^{-1} .^[21,43,44] Based on reactions with (partially) deuterated reactants, these experiments suggested only the formation of phenylallene ($C_6H_5CHCCH_2$) and 1-phenyl-1-propyne (CH_3CCCH_3), respectively. The authors concluded that the lifetimes of the initial collision complexes were too short to allow successive isomerization steps, such as hydrogen shift(s) and ring closures, to form indene under single-collision conditions. These results are in line with previous electronic structure calculations at the B3LYP/6-311+G** level of theory (Figure 1).^[45–47] Vereecken et al. were able to estimate the formation of indene versus phenyl with side-chain products.^[45,46] Indene formation favors temperatures below 1000 K and moderate pressures. At combustion temperatures between 1000 and 2000 K and at pressures of 1 to 100 atm, indene plus a hydrogen atom was found to account for only 5% of the products, although Vereecken et al. admitted this was subject to major errors owing to the branching ratios being sensitive to collisional transfer processes, especially for stabilized versus dissociated products. Because

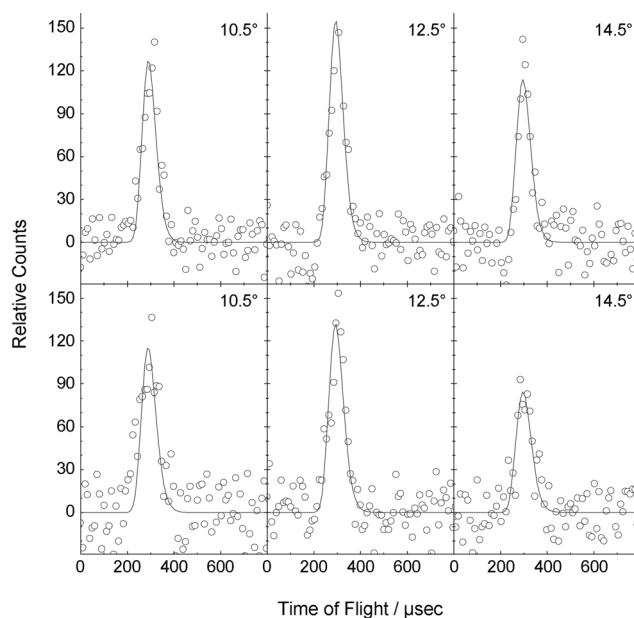


Figure 1. Top: Time-of-flight (TOF) data for the reaction of the $[D_3]$ phenyl radical (C_6D_5 , X^2A_1) with $[D_4]$ allene (D_2CCCD_2 , X^1A_1) monitored at m/z 124. Bottom: TOF data for the reaction of the $[D_3]$ phenyl radical (C_6D_5 , X^2A_1) with $[D_4]$ methyl acetylene (CD_3CCD , X^1A_1) monitored at m/z 124.

no experimental data existed at that time, there was no way to calibrate these parameters effectively.

Herein, we investigate the reactions of a phenyl radical with allene and methylacetylene, together with their (partially) deuterated counterparts, under single-collision conditions at collision energies of 43.4–47.3 kJ mol⁻¹, which are about 40 to 120 kJ mol⁻¹ lower than previous studies by our group. The reduced collision energy should be reflected in a prolonged lifetime of the initial collision complex, so that the initially formed intermediates might isomerize to eventually form the aromatic indene molecule. Finally, we recalculated the relevant pathways to form indene and its non-PAH isomers theoretically and merged these data with crossed-molecular-beam studies to gain a unified understanding of the synthesis of the polycyclic aromatic indene molecule under single-collision conditions.

Results

Laboratory Data

Initially, our goal was to conduct scattering experiments of the phenyl radical (C₆H₅; X²A₁) with allene (H₂CCCH₂) and methylacetylene (CH₃CCH) to investigate the formation of various C₉H₈ isomers (*m/z* 116), including indene. However, we observed background interference from nonreactively scattered, nonphotolyzed ¹³C₂C₄H₅³⁷Cl (*m/z* 116), which arose from the naturally occurring, doubly ¹³C-substituted chlorobenzene precursor. Therefore, we decided to conduct experiments with fully deuterated reactants to overcome this background problem. For the reactions of deuterated phenyl radicals (C₆D₅; X²A₁) with [D₄]methylacetylene (CD₃CCD; X¹A₁) and [D₄]allene (D₂CCCD₂; X¹A₁), a reactive scattering signal was detected at *m/z* 124, which corresponded to a molecule with an empirical formula C₉D₈. This finding alone demonstrates the formation of C₉D₈ isomer(s) plus atomic deuterium in both systems. Selected TOF spectra are shown in Figure 1. Note that no molecular deuterium elimination channel was observed. Fits of the TOF spectra for both systems were conducted by using a single channel with a mass combination of 124 amu (C₉D₈) and 2 amu (D), utilizing identical center-of-mass functions. The TOF spectra at each angle were also integrated and scaled according to the number of scans to derive the laboratory angular distribution (LAB) of the C₉D₈ products at the most intense *m/z* value of 124 (C₉D₈) (Figure 2). Both LAB distributions are spread over about 20° in the scattering plane defined by the [D₅]phenyl radical and hydrocarbon reactant beams. Furthermore, the LAB distributions are forward-backward symmetric; these observations imply that both reactions are likely to proceed through indirect (complex forming) scattering dynamics involving C₉D₉ reaction intermediate(s). It should be stressed that the most significant difference between the [D₄]allene and [D₄]methylacetylene reactants was the intensity of the signal upon reaction with [D₅]phenyl at *m/z* 124. At all angles, the ion counts for C₉D₈⁺ were consistently stronger by about 20% for the [D₄]allene reactant.

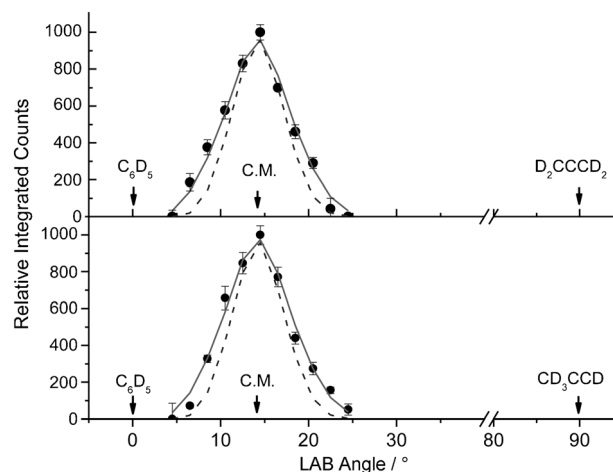


Figure 2. Top: Laboratory angular distribution (LAB) of the C₉D₈ reaction product recorded at *m/z* 124 by reaction of the [D₅]phenyl radical (C₆D₅ X²A₁) with [D₄]allene. Bottom: LAB of the C₉D₈ reaction product recorded at *m/z* 124 by reaction of the [D₅]phenyl radical (C₆D₅ X²A₁) with [D₄]methylacetylene. Circles signify experimental data, the line denotes best fit data, and the dashed line indicates best fit data with an exoergic of the monocylic C₉D₈ isomer 1-phenylpropyne of 89 kJ mol⁻¹. C.M. indicates the center-of-mass angle.

So far we have established that the reactions of the [D₅]phenyl radical with [D₄]allene and [D₄]methylallene form C₉D₈ isomer(s) under single-collision conditions. However, it is important to elucidate if the deuterium originated from the [D₅]phenyl radical and/or from the [D₄]hydrocarbon; the deuterium atoms of the methyl and acetylenic groups of methylacetylene are not equivalent. To answer these questions, we conducted cross-beam experiments at the center-of-mass angle for the reaction of phenyl and [D₅]phenyl radicals with deuterated and partially deuterated allene and methylacetylene (see Table S2 in the Supporting Information). In the reactions of [D₅]phenyl with [D₃]methylacetylene (CD₃CCH) and [D₁]methylacetylene (CH₃CCD), the hydrogen atoms can only be released from the acetylenic and methyl groups, respectively. We observed scattering signals at *m/z* 124 (C₉D₈⁺) and 122 (C₉D₆H₂⁺), respectively, indicating that the hydrogen atom was lost from the methyl group and from the acetylenic group (Figure 3) with reactive scattering signals of similar intensity for both systems at the center-of-mass angles. We also performed scattering experiments of phenyl radicals (C₆H₅) with [D₄]allene and [D₄]methylacetylene to investigate to what extent hydrogen atoms were lost from the aromatic phenyl ring. Here, weak reactive scattering signal was observed at *m/z* 120 for both systems (C₉D₄H₄⁺). The intensity of the signal for the hydrogen atom lost from the phenyl group, however, was significantly smaller and only reached levels of 10% relative to the signal observed for hydrogen loss monitored in the [D₅]phenyl reactions with [D₃]methylacetylene (CD₃CCH) and [D₁]methylacetylene (CH₃CCD). Therefore, we have to conclude that the signal at *m/z* 120 observed in both reactions was unlikely to originate from atomic hydrogen loss from the phenyl ring form-

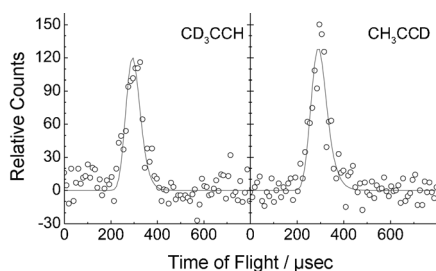


Figure 3. Center-of-mass time-of-flight data for the reaction of the $[D_5]$ phenyl radical (C_6D_5 , X^2A_1) with partially deuterated methyl acetylene CH_3CCD (X^1A_1) and CD_3CCH (X^1A_1) monitored at m/z 122 and 124, respectively.

ing $C_9D_4H_4$ within the errors of our counting system, but rather from the naturally occurring ^{13}C isotopically substituted $^{13}CC_8H_5D_3$ synthesized by atomic deuterium loss. Note that $^{13}CC_8H_5D_3$ is formed at concentrations of about 9.9% relative to $C_9H_5D_3$; therefore, counts at m/z 120 are within our error limits and are the result of naturally occurring $^{13}CC_8H_5D_3$, and not from $C_9H_4D_4$ isomers formed. Therefore, we may conclude that the emission of a hydrogen atom from the phenyl ring—if present—is a minor process at most.

To summarize, laboratory data depict the following results: First, the reactive scattering signal of m/z 124 ($C_9D_8^+$) in the reaction with $[D_4]$ allene and $[D_4]$ methylacetylene suggests the formation of C_9D_8 isomers by atomic deuterium loss with a scattering signal enhanced by about 20% for the $[D_4]$ allene reactant relative to $[D_4]$ methylacetylene. Second, reactions with partially deuterated reactants indicated that, in the corresponding reactions with perdeuterated reactants, deuterium loss originated—within the limits of our detection system—from the C3-hydrocarbons (methylacetylene, allene), and not from the phenyl radical. Finally, experiments with $[D_3]$ - and $[D_1]$ methylacetylene provided evidence of two exit channels: emission of atomic hydrogen from the methyl and from the acetylenic group.

Center-of-Mass Frame

Having identified the molecular mass of the reaction product(s) (m/z 124), and hence, an empirical formula of C_9D_8 for the reaction of the $[D_5]$ phenyl radical with both C_3D_4 isomers, and having established that the deuterium elimination originates from the C_3D_4 molecule, we attempted to extract information on the underlying reaction dynamics. This was achieved by converting the laboratory data into the center-of-mass reference frame and analyzing the resulting center-of-mass angular $T(\theta)$ and translational energy $P(E_T)$ distributions. The simulated distributions (TOF, laboratory angular distribution) are overlaid on the experimental data in Figures 1 and 2 with their corresponding center-of-mass functions visualized in Figure 4. It is important to stress that both data sets for the allene and methylacetylene systems could be fit with identical, one-channel center-of-mass functions. We turned our attention first to the derived center-of-

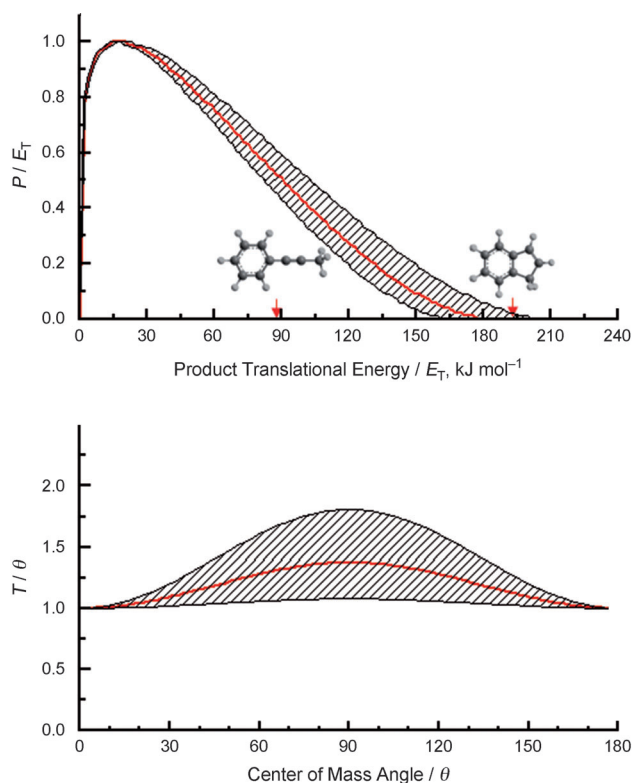


Figure 4. Center-of-mass translational energy flux distribution (upper) and angular distribution (lower) utilized to fit data at m/z 124 in the reactions of $[D_5]$ phenyl radicals with $[D_4]$ allene and $[D_4]$ methylacetylene. Hatched areas indicate the acceptable upper and lower error limits of the fits and the red line defines the best-fit function.

mass translational energy distribution, $P(E_T)$ (Figure 4). The high-energy cutoff of $P(E_T)$ represented the sum of the absolute reaction exoergicity and the collision energy. Subtracting the collision energy of (46 ± 2) kJ mol^{-1} from the high energy cutoff of (177 ± 25) kJ mol^{-1} yielded a reaction exoergicity of (131 ± 25) kJ mol^{-1} to form the C_9D_8 isomer plus atomic deuterium. Second, the $P(E_T)$ has a distribution maximum at 12–20 kJ mol^{-1} , which indicated the existence of a rather tight exit transition state. According to the principle of microscopic reversibility of a chemical reaction, the reverse reaction of a deuterium atom adding to the C_9D_8 molecule should have an entrance barrier; this finding indicates that the deuterium atom adds either to a carbon-carbon double, triple, or aromatic bond of a closed-shell hydrocarbon.^[48] Finally, we determined the fraction of energy channeling into the translational modes of the products to be about $(31 \pm 4)\%$ for both systems; a comparison of this order of magnitude with previous crossed-beam data reflects indirect scattering dynamics^[48] involving C_9D_9 collision complex(es).

Having interpreted the center-of-mass translational energy distribution, we then analyzed the information provided in the center-of-mass angular distribution. Here, the center-of-mass angular distribution, $T(\theta)$, displays an intensity over the complete angular range, indicating C_9D_9 com-

plex formation, and hence, indirect scattering for both the $[D_4]$ allene and $[D_4]$ methylacetylene reactions.^[49] The forward-backward symmetry further indicates a lifetime of the decomposing complex(es) longer than the (ir) rotation period(s). Finally, the best-fit distribution depicts a pronounced maximum at 90° (Figure 4) with a ratio of the fluxes at the respective maxima and minima $I(90^\circ)/I(0^\circ)$ of (1.8 ± 0.3) . The shape of this angular distribution strongly suggests geometrical constraints when the C_9D_9 intermediate decomposes to the final products.^[50] In this case, atomic deuterium elimination occurs perpendicularly to the molecular plane of the rotating, decomposing intermediate and almost parallel to the total angular momentum vector of the system. Note that this 'sideways' scattering is reflected in the flux contour plot (Figure 5). Since the center-of-mass translational energy distributions and the center-of-mass angular distributions are identical in both systems, we suggest that the molecular structures of the dominating C_9D_9 intermediate forming the C_9D_8 product plus atomic deuterium are the same in both reactions.

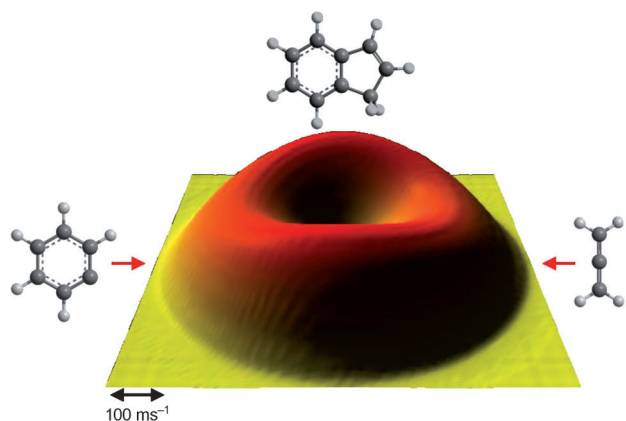


Figure 5. Flux contour map of the reaction of $[D_5]$ phenyl radicals ($C_6D_5 X^2A_1$) with $[D_4]$ methyl acetylene and $[D_4]$ allene to form $[D_8]$ indene and atomic deuterium at collision energies of 46.3 and 46.4 kJ mol^{-1} , respectively.

Discussion

Product Isomer Identification

The reactive scattering signal for the reactions of phenyl radicals with methylacetylene and allene indicates the formation of C_9D_8 isomer(s) plus atomic deuterium. By considering the energetics of the reaction, we attempted to elucidate the nature of the product isomer(s) formed in these reactions. Here, we compared the experimentally determined reaction exoergicity of $(131 \pm 25) \text{ kJ mol}^{-1}$ with the theoretically predicted energetics for distinct isomers (Figure 6). Note that the energetics in Figure 6 are given for undeuterated reactants; the energetics for the (partially) deuterated reactants change only by the differences in zero-point energies (ZPEs), which are in the order of 5–10 kJ mol^{-1} for the systems considered in the present study and falls within the

error limits of our study. In the case of undeuterated products, the reaction exoergicities to yield indene from methylacetylene and allene are (-148 ± 8) and $(-153 \pm 8) \text{ kJ mol}^{-1}$, respectively. These data agree nicely with our experimental value of $(131 \pm 25) \text{ kJ mol}^{-1}$ within error limits. The thermodynamically closest isomer to $[D_8]$ indene is the $[D_8]$ 1-phenyl-1-propyne molecule (Figure 6). This isomer is 110 kJ mol^{-1} less stable than indene; its formation would result in reaction energies of (-38 ± 8) and $(-43 \pm 8) \text{ kJ mol}^{-1}$ for $[D_4]$ methylacetylene and $[D_4]$ allene, respectively. Adding the collision energy, this isomer is marked at -89 kJ mol^{-1} in Figure 4. The fits of the corresponding laboratory angular distribution indicated by dashed blue lines—assuming an available energy of 89 kJ mol^{-1} —are inadequate and too narrow relative to the laboratory data (Figure 2). Therefore, based on the energetics, we can conclude that for both systems, at least the thermodynamically most stable $[D_8]$ indene isomer is formed. However, at present, we cannot exclude smaller fractions of the thermodynamically less stable isomers compiled in Figure 6.

Proposed Reaction Dynamics

Having provided evidence for the formation of at least the aromatic $[D_8]$ indene molecule in both reactions, we turned our attention to the elucidation of the reaction dynamics. For this, we correlated the structure of the indene reaction product with the reactants and interpreted the experimental data in terms of the underlying potential energy surfaces (Figure 6).

$[D_5]$ Phenyl- $[D_4]$ Allene

First, let us consider the $[D_5]$ phenyl- $[D_4]$ allene system (Figure 6). The calculations suggest that the $[D_5]$ phenyl radical can add to one of the terminal (C1/C3) or central (C2) carbon atoms of the $[D_4]$ allene molecule to form two radical intermediates: Rad 11 and Rad 6, respectively. The entrance barriers of these addition processes of 1 and 15 kJ mol^{-1} are well below our collision energies of 43–47 kJ mol^{-1} (Table S2 in the Supporting Information), and hence, can be overcome easily. Considering the lower barrier to C1/C3 addition and the statistical factor of the number of carbon atoms to be attacked, the addition to one of the terminal carbon atoms should be preferred. Rad 11 then undergoes a deuterium shift from the *ortho* position of the $[D_5]$ phenyl group to the C2 position of the $[D_4]$ allene moiety to yield Rad 21. The latter undergoes ring closure to form Rad 22, which can then only eliminate a deuterium atom from the C1 or C3 atoms of the former allene moiety to yield the $[D_8]$ indene molecule via a tight exit transition state. Our experimental results fully support this pathway. First, the corresponding center-of-mass angular distribution suggests indirect scattering dynamics involving decomposing C_9D_9 complexes. This complex can be identified as Rad 22. Furthermore, geometrical constraints of the deuterium atom emissions were predicted based on the center-of-mass angular distribution. The geometry of the exit transition state depicts that the deuteri-

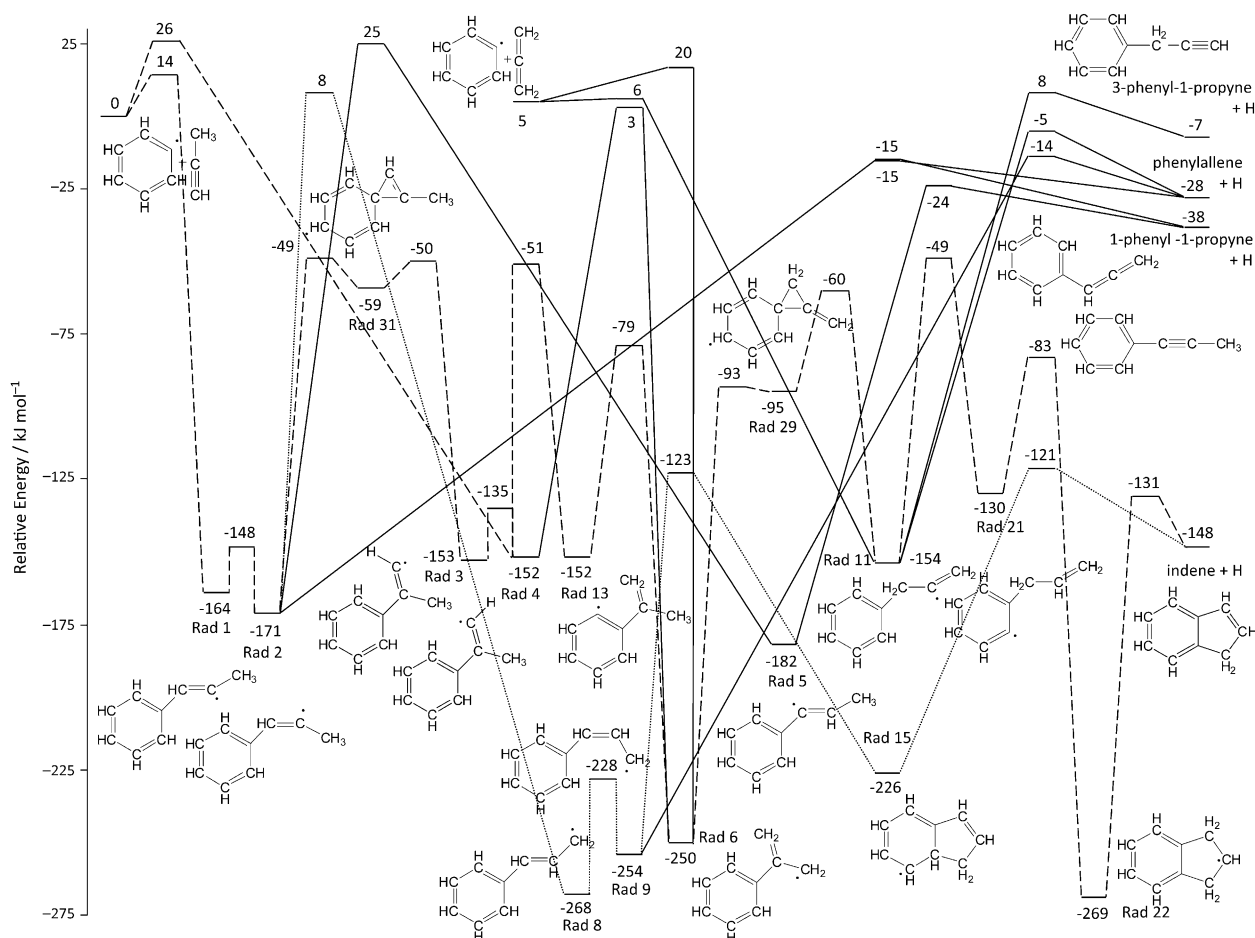


Figure 6. Potential energy surface for the reactions of $[D_5]$ phenyl radicals with $[D_4]$ allene and $[D_4]$ methylacetylene. All relative energies (in kJ mol^{-1}) are calculated at the G3(MP2,CC)//B3LYP/6-311+G**+ZPE(B3LYP/6-311+G**) level of theory. The labels of the reaction intermediates Rad were taken from references [46–48].

um atom is emitted almost parallel to the total angular momentum vector, and hence, nearly perpendicularly to the rotation plane of the decomposing complex at an angle of 77.6° (Figure 7). In the reverse reaction, the deuterium atom adds to the aromatic system almost perpendicularly to the molecular plane of the $[D_8]$ indene molecule. The deuterium atom therefore approaches on axis to the HOMO to gain full overlap, and hence, complete the bonding. The extent to which the deuterium emission would be preferentially per-

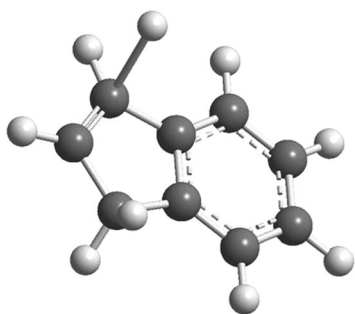


Figure 7. Structure of the transition state of the decomposing Rad 22 intermediate that forms $[D_8]$ indene and atomic deuterium (from Ref. [48]).

pendicular to the principal rotation axis would be expected to be less in the monocyclic isomers than that in $[D_8]$ indene. Previous cross-beam experiments for the formation of the non-PAH product isomers 1-phenyl-1-propyne, phenylallene, and 3-phenyl-1-propyne found no maximum at 90° in the center-of-mass angular distributions.^[21,43] Since the proposed pathway represents the addition of a deuterium atom to a closed-shell aromatic system, we would also expect an entrance barrier. This barrier has been computed to be about 17 kJ mol^{-1} . Recall that the nature of a tight exit transition state was also predicted based on the center-of-mass translational energy distribution maximum at $12\text{--}20 \text{ kJ mol}^{-1}$. Note that if Rad 6 is formed by the addition of $[D_5]$ phenyl to the central carbon atom of $[D_4]$ allene, this intermediate eventually isomerizes through $[D_5]$ phenyl group shift from Rad 29 to Rad 11. Therefore, both initial addition pathways yield the $[D_8]$ indene molecule plus atomic deuterium through indirect scattering dynamics.

Can these findings also explain the failed detection of the hydrogen elimination pathway in the phenyl- $[D_4]$ allene system? If phenyl adds to $[D_4]$ allene, this would result in Rad 6 and Rad 11 in which all hydrogen atoms are initially on the phenyl group (Figure 8). A hydrogen shift in Rad 11

from the phenyl group would result in Rad 21 with the shifted hydrogen atom being located at the C2 atom of the former [D₄]allene moiety. The cyclization to Rad 22 would yield an intermediate with four hydrogen atoms at the former phenyl ring and a single hydrogen atom at the central carbon atom of the former [D₄]allene molecule. Indene can only be formed by deuterium elimination from the C1/C3 carbon atom of the incorporated allene moiety. Therefore, the experimental lack of any atomic hydrogen loss pathway can be fully accounted for by the reaction mechanism proposed above.

Finally, we would like to discuss the possibility of forming nonaromatic C₉D₈ isomers. Deuterium elimination from C1 and C3 of Rad 11 could also lead to [D₈]phenylallene and [D₈]3-phenyl-1-propyne, respectively, in less exoergic reactions (−28 and −7 kJ mol^{−1}). Based on our considerations above, the formation of smaller fractions of these isomers cannot yet be excluded. To untangle the final piece of the puzzle, we conducted Rice–Ramsperger–Kassel–Marcus (RRKM) calculations (Table 1). These calculations suggested that once Rad 6 and Rad 11 formed, the indene isomer was almost an exclusive product (more than 98%) via decomposition of Rad 22 at collision energies up to 50 kJ mol^{−1}. Note that [D₈]indene could also result from fragmentation of Rad 15 by emitting a deuterium atom from the bridged carbon atom. However, Rad 15 cannot be accessed in the reaction of [D₅]phenyl with [D₄]allene. [D₈]Phenylallene and [D₈]3-phenyl-1-propyne were predicted to be formed at levels less than 2%. However, previous crossed-beam experiments with phenyl radicals and hydrocarbons for collision energies in the range 91–161 kJ mol^{−1}[21,43] suggested that, in the case

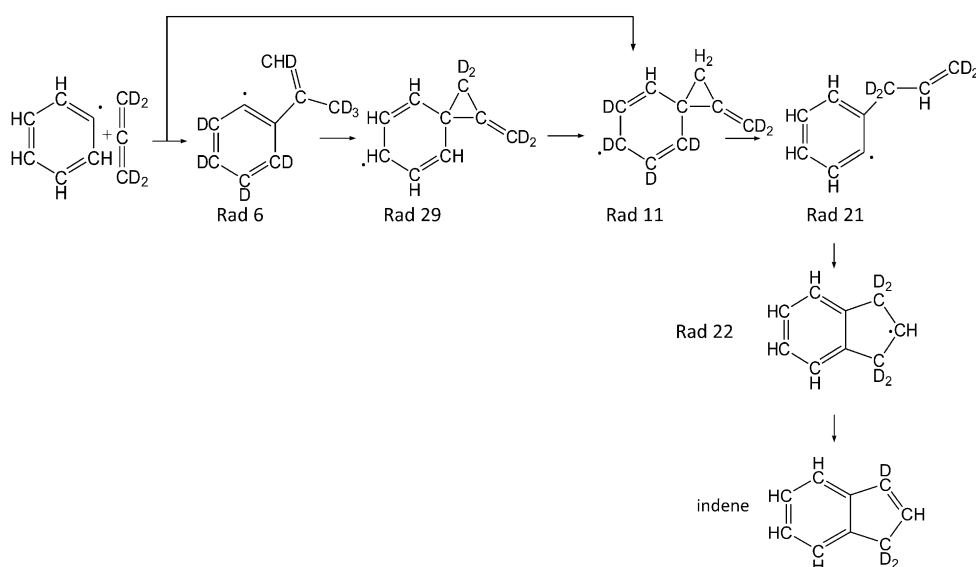


Figure 8. Flow diagram of the reaction pathway for the reaction of phenyl with [D₄]allene.

Table 1. Product branching ratios [%] in the reactions of phenyl radicals with methylacetylene and allene calculated using RRKM theory at various collision energies.

Product	Collision energy [kJ mol ^{−1}]						
	0.00	10.00	20.00	30.00	40.00	50.00	60.00
C₆H₅+CH₃CCH → Rad 1							
3-phenyl-1-propyne+H	1.07 × 10 ^{−8}	3.29 × 10 ^{−5}	0.00	0.01	0.04	0.10	0.24
phenylallene+H	0.06	0.24	0.64	1.36	2.44	3.90	5.67
1-phenyl-1-propyne+H	0.16	0.63	1.71	3.62	6.49	10.32	14.93
indene+H (total)	99.78	99.13	97.65	95.01	91.03	85.68	79.17
indene+H (from Rad 15)	3.67 × 10 ^{−7}	1.03 × 10 ^{−3}	2.75 × 10 ^{−3}	6.52 × 10 ^{−3}	1.34 × 10 ^{−2}	2.45 × 10 ^{−2}	4.02 × 10 ^{−2}
indene+H (from Rad 22)	99.78	99.13	97.65	95.01	91.02	85.65	79.13
C₆H₅+CH₂CCH₂ → Rad 6							
3-phenyl-1-propyne+H	1.07 × 10 ^{−8}	3.31 × 10 ^{−5}	0.00	0.01	0.04	0.12	0.28
phenylallene+H	0.01	0.05	0.14	0.31	0.59	1.00	1.52
1-phenyl-1-propyne+H	0.03	0.12	0.34	0.76	1.41	2.31	3.43
indene+H (total)	99.96	99.83	99.52	98.92	97.96	96.58	94.77
indene+H (from Rad 15)	6.28 × 10 ^{−8}	1.92 × 10 ^{−4}	5.48 × 10 ^{−4}	1.37 × 10 ^{−3}	2.92 × 10 ^{−3}	5.48 × 10 ^{−3}	9.22 × 10 ^{−3}
indene+H (from Rad 22)	99.96	99.83	99.52	98.92	97.95	96.57	94.76
C₆H₅+CH₂CCH₂ → Rad 11							
3-phenyl-1-propyne+H	1.07 × 10 ^{−8}	3.32 × 10 ^{−5}	0.00	0.01	0.04	0.12	0.29
phenylallene+H	0.01	0.03	0.10	0.23	0.44	0.74	1.14
1-phenyl-1-propyne+H	0.02	0.09	0.24	0.54	0.99	1.61	2.36
indene+H (total)	99.97	99.88	99.65	99.22	98.52	97.53	96.21
indene+H (from Rad 15)	4.62 × 10 ^{−8}	1.40 × 10 ^{−4}	3.95 × 10 ^{−4}	9.74 × 10 ^{−4}	2.06 × 10 ^{−3}	3.82 × 10 ^{−3}	6.36 × 10 ^{−3}
indene+H (from Rad 22)	99.97	99.88	99.65	99.22	98.52	97.52	96.21

of the allene reaction, the phenylallene molecule presents the exclusive product formed. Kaiser et al. [21,43] interpreted these findings in terms of a short-lived reaction intermediate, in which the full energy randomization was rather in-

complete. This short lifetime effectively prohibited successive isomerization steps of Rad 11 and led to instantaneous emission of atomic deuterium from the C1-position, yielding phenylallene.

[D₅]Phenyl–

[D₄]Methylacetylene

Electronic structure calculations predicted that the [D₅]phenyl radical added preferentially to the sterically less hindered C1 carbon atom of the [D₄]methylacetylene molecule, forming a Rad 1 collision complex (Figure 6). Similar to the [D₅]phenyl–[D₄]allene system, the barrier to addition of 14 kJ mol⁻¹ can be overcome in our experiments when considering our collision energies of 43–47 kJ mol⁻¹ (Table S2 in the Supporting Information). Upon *cis/trans* isomerization, two pathways exist for Rad 2 to form [D₈]indene. These are visualized in Figure 6 as dashed (low-energy pathway) and dotted (high-energy pathway) lines. The low-energy pathway involves [D₅]phenyl group migration from the C1 to the C2 carbon atom of the [D₄]methylacetylene moiety to form Rad 3 via Rad 31; Rad 3 then undergoes *cis/trans* isomerization. A deuterium shift from the *ortho* position of the phenyl group to the C1 position of the C3 unit yields Rad 13. This intermediate isomerizes by a deuterium shift to Rad 6, which in turn undergoes various isomerizations to form [D₈]indene, as discussed in the previous section on the [D₅]phenyl–[D₄]allene system. The high-energy pathway involves a deuterium shift within the methylacetylene unit to form Rad 8 from Rad 2. The former undergoes *cis/trans* isomerization followed by cyclization to form Rad 15 and successive deuterium loss leads to [D₈]indene. Based on the experimental results of the [D₅]phenyl–[D₄]methylacetylene system alone we cannot discriminate between these pathways explicitly. However, the barrier of 27 kJ mol⁻¹ for the tighter exit transition state from Rad 15 to form [D₈]indene plus atomic deuterium is less supported by the distribution maximum of the center-of-mass translational energy distribution maximum at mild energies of 12–20 kJ mol⁻¹. Therefore, the experimental data indicates that the energetically favorable pathway dominates. Note that, to a minor extent, theory predicts that the [D₅]phenyl radical can add to the C2 carbon atom of [D₄]methylacetylene to yield Rad 4 in one step.

However, can the reactions of [D₅]phenyl with [D₃]– and [D₁]methylacetylene or phenyl with [D₄]methylacetylene shed light on this open question? Figure 9 depicts the partially deuterated intermediates formed in the phenyl–[D₄]methylacetylene system for the high-energy pathway. Here, a deuterium shift in the [D₄]methylacetylene moiety in Rad 2 yields Rad 8, which—after *cis/trans* isomerization

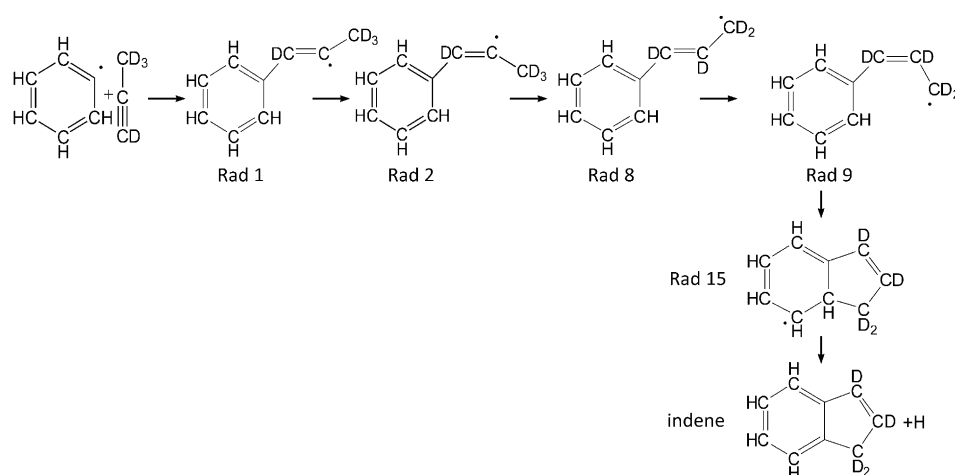


Figure 9. Flow diagram of the high-energy reaction pathway for reaction of phenyl with [D₄]methylacetylene.

to Rad 9—ring closes to form Rad 15. This intermediate can only decompose by atomic hydrogen loss, and not by emission of atomic deuterium, to the indene molecule. This hydrogen atom must be released from the bridged carbon atom in Rad 15 (Table 1). However, because we did not observe any atomic hydrogen elimination in the phenyl–[D₄]methylacetylene system, we have to conclude that the high-energy pathway is—at least within the detection limits of our system—not accessible. As a matter of fact, our RRKM calculations fully support this conclusion: once Rad 1 is formed under single-collision conditions, indene is predicted to form practically exclusively via decomposition of Rad 22, and not via Rad 15. Therefore, our experiments of the phenyl radicals with [D₄]methylacetylene provide solid evidence that the indene molecule cannot be formed through the high-energy pathway involving the decomposition of Rad 15; therefore, we can eliminate this pathway from further considerations.

A closer look at the reactions of [D₅]phenyl with [D₃]– and [D₁]methylacetylene exposes further details for the low-energy pathway to form indene (Figures 10 and 11). Figure 10 compiles the resulting intermediates accessible in the reaction with [D₃]methylacetylene and the experimentally observed atomic hydrogen loss. Starting with the addition of the [D₅]phenyl radical to the C1 carbon atom of [D₃]methylacetylene, the intermediate formed (Rad 1) undergoes rapid *cis/trans* isomerization to Rad 2. The latter is involved in a [D₅]phenyl group migration through intermediate Rad 31 to form Rad 3 and then Rad 4 after *cis/trans* isomerization. This intermediate undergoes deuterium transfer from the *ortho* position of the [D₅]phenyl group to form Rad 13, which then undergoes another deuterium migration from the [D₅]phenyl group of the former methylacetylene reactant to form Rad 6. In Rad 6, the [D₅]phenyl group can migrate either to the CHD or CD₂ moieties of the C3 side chain involving Rad 29 to form two isotopologues of Rad 11. Both structures isomerize through a deuterium shift from the [D₅]phenyl group to the central carbon atom of the C3 group, forming two distinct isotopologues of Rad 21,

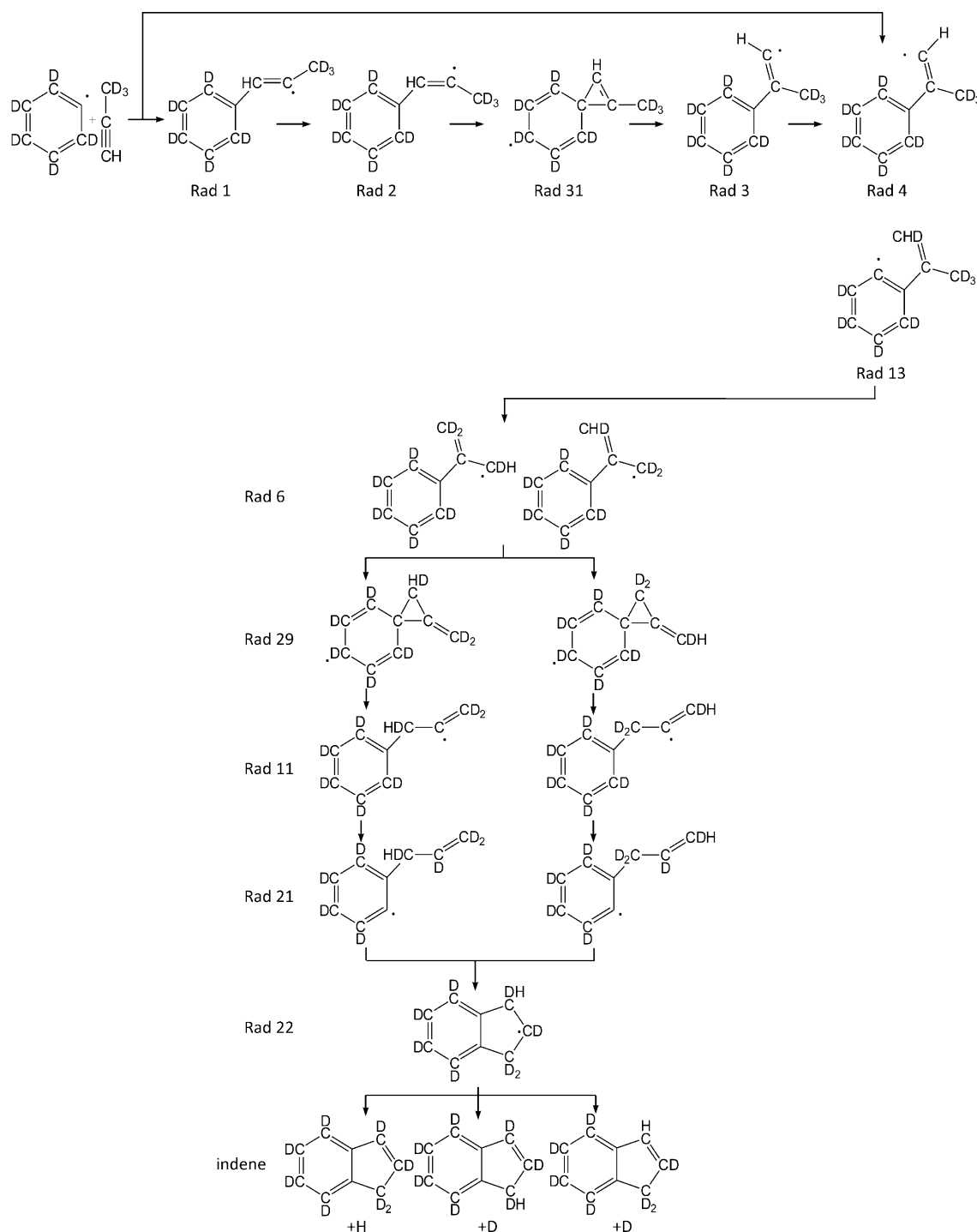


Figure 10. Flow diagram of the low-energy reaction pathway for reaction of $[D_5]$ phenyl radicals with $[D_3]$ methylacetylene.

which can then ring close to form Rad 22. Indene formation can proceed by deuterium or hydrogen emission from the CD_2 , CDH (deuterium elimination), or from CDH groups (hydrogen elimination). Therefore, the experimentally observed atomic hydrogen loss can be rationalized in terms of the formation of $[D_8]$ indene from Rad 22.

The $[D_5]$ phenyl– $[D_1]$ methylacetylene system follows a similar pattern (Figure 11). Initiated by the addition of the

$[D_5]$ phenyl radical to the C1 carbon atom of methylacetylene, Rad 1 undergoes *cis/trans* isomerization to form Rad 2. Similar to the system discussed above, Rad 2 undergoes $[D_5]$ phenyl group migration via intermediate Rad 31 to yield Rad 3 and eventually Rad 4. Rad 4 isomerizes by deuterium migration from the *ortho* position of the $[D_5]$ phenyl group to Rad 13, followed by a hydrogen atom shift from the phenyl group to form Rad 6. In Rad 6, the $[D_4]$ phenyl group

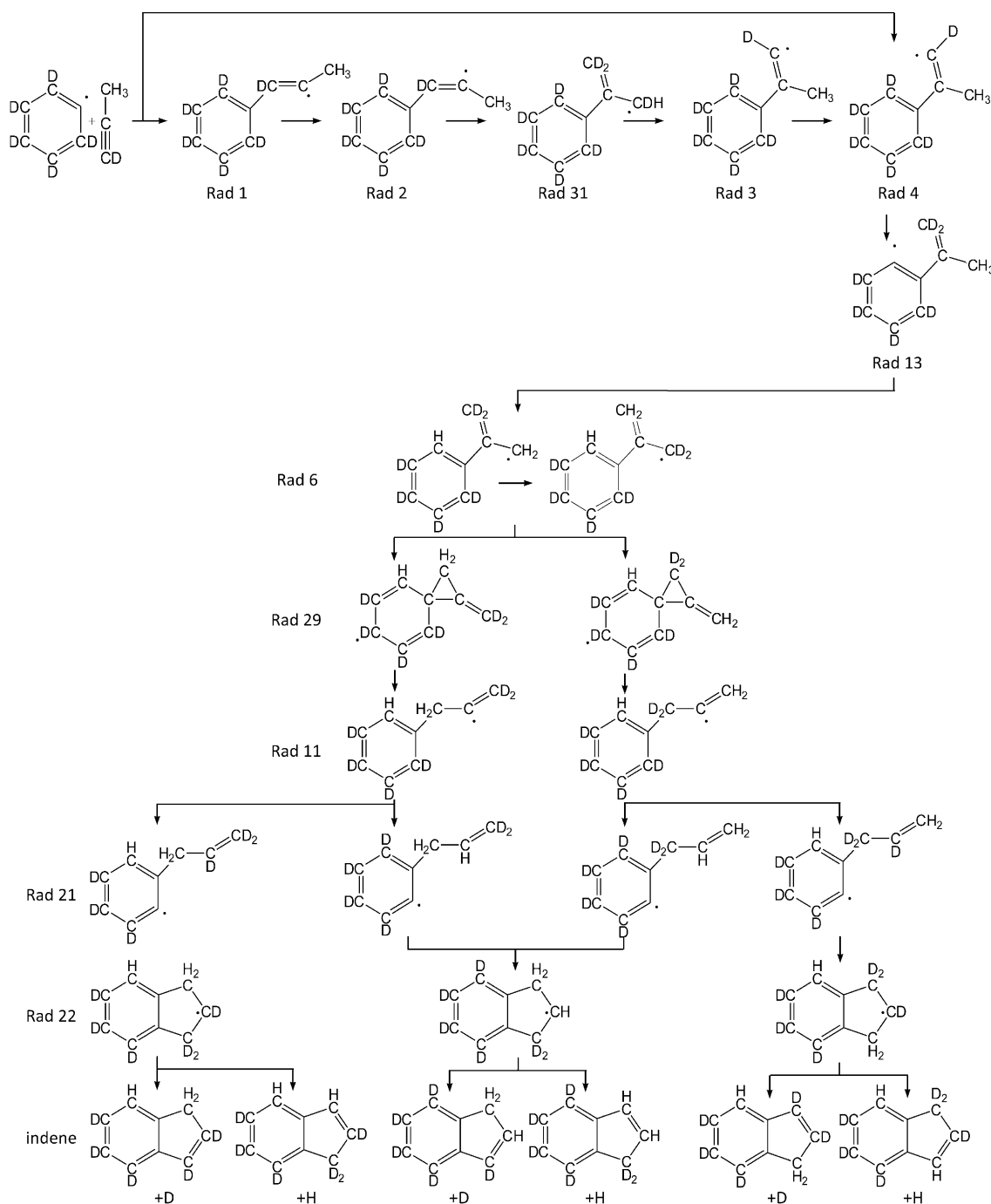


Figure 11. Flow diagram of the low-energy reaction pathway for reaction of [D₃]phenyl radicals with [D₁]methylacetylene.

migrates to either the CH₂ or CD₂ groups of the C3 side chain via Rad 29 to form two distinct isotopologues of Rad 11. Both intermediates can isomerize by a hydrogen or deuterium shift from the *ortho* position of the [D₄]phenyl group to the central carbon atom of the C3 group to form a total of four distinct isotopologues of Rad 21, which can then ring close to form three distinct isotopologues of Rad 22. A total of six isotopologues of indene can be formed through atomic hydrogen and deuterium loss pathways, as compiled in Figure 11. Therefore, the experimental-

ly detected hydrogen atom loss can account for the formation of [D₆]indene from Rad 21 (emission from the CH₂ group) in each case.

We also conducted a theoretical investigation of the phenyl–methylacetylene system by RRKM studies (Table 1). Here, main results are that the indene molecule presents the dominant reaction product with fractions of about 98% decreasing to around 85% by increasing the collision energy from 20 to 50 kJ mol⁻¹. To a minor extent, 1-phenyl-1-propyne (2–10%) and phenylallene (0 to ≈5%) can be also

formed. Recall that, at elevated collision energies, from 91.4 to 161 kJ mol⁻¹,^[21,43] of phenyl radicals with hydrocarbons, detailed experiments with isotopically labeled reactants suggested the exclusive formation of 1-phenyl-1-propyne. Once again, the lifetime of the reaction intermediate at these high collision energies does not allow complete energy randomization, and hence, successive isomerization steps of the initial collision complexes, but rather rapid fragmentation of the collision complexes to form 1-phenyl-1-propyne (Figure 6).

Conclusion

In our laboratory, reactions of the [D₅]phenyl radical with [D₄]allene and [D₄]methylacetylene, together with their (partially) deuterated counterparts, were studied under single-collision conditions at collision energies of around 45 kJ mol⁻¹. Experimental data were combined with electronic structure calculations. Our experiments provided, for the first time, compelling evidence that an individual PAH—herein the [D₈]indene molecule—could be formed as a result of a single collision event in the gas phase. The experimental finding of essentially indistinguishable center-of-mass angular and translational energy distributions for both systems can be understood in terms of the derived reaction mechanism, which involved the decomposition of an identical reaction intermediate, Rad 22, in both systems to form [D₈]indene by atomic deuterium loss through a tight exit transition state located about 17 kJ mol⁻¹ above the separated products. The experimentally observed geometrical constraints of a preferential sideways scattering, that is, the ejection of a deuterium atom from the decomposing intermediate almost perpendicularly to the rotation plane, could be verified theoretically and suggested that the deuterium atom left at an angle of 77.6° with respect to the principal rotation axis. Considering the [D₄]allene reaction, Rad 11 was identified as the central reaction intermediate formed by either addition of the [D₅]phenyl radical to the C1 carbon atom of [D₄]allene or one-step isomerization starting with Rad 6. Rad 6 was also accessed in the reaction of [D₅]phenyl with [D₄]methylacetylene, which involved a six-step isomerization sequence of the initial collision complex Rad 1. Both reactions therefore ultimately yielded Rad 11, which rearranged to form Rad 22 in two steps. The latter undergoes deuterium loss to form the [D₈]indene molecule under single-collision conditions.

We would like to add that we also attempted to re-fit our data at higher collision energies up to 161 kJ mol⁻¹ for the phenyl radical plus allene and methylacetylene reactions disseminated earlier.^[21,43,44] Assuming that the $P(E_T)$ values in the present experiments (low collision energy) were solely from the formation of indene plus atomic hydrogen and that the $P(E_T)$ values in our previous studies (high collision energies) originated solely from acyclic isomers, we utilized a two-channel fit (channel 1: indene; channel 2: acyclic isomers) for the high-energy TOF and LAB distributions. We

could typically add a contribution of (15 ± 5)% of the indene channel without changing the outcomes of the fit. Therefore, within the limits of the two-channel fits discussed above, up to (15 ± 5)% of the indene might be formed at higher collision energies. However, we have to stress that the original fits, without any contribution of indene, can also replicate the experimental data. To summarize, we can conclude that the indene molecule can be easily formed in combustion flames and in high-temperature regions of circumstellar envelopes (a few 1000 K) and (pre)planetary nebulae as a result of a single collision event. However, the entrance barriers block the formation of indene in cold molecular clouds, where averaged translational temperatures of the reactants of 10 K cannot overcome entrance barriers as low as 1 kJ mol⁻¹. We hope that this experimental protocol can act as a template to elucidate the formation of more complex PAHs, such as naphthalene, under single-collision conditions at collision energies low enough to allow cyclization and involving the reaction of phenyl radicals with hydrocarbon molecules, and thus, determine the likelihood of PAH formation in combustion and space environments.

Experimental Section

Experiments were carried out under single-collision conditions in a crossed-molecular-beam machine at the University of Hawaii.^[52] Briefly, a molecular beam of (deuterated) phenyl radicals (C₆H₅, C₆D₅; X²A₁) seeded in helium (99.9999%; Gaspro) at fractions of about 1% was prepared by photolysis of (deuterated) chlorobenzene (C₆H₅Cl 99.9%; C₆D₅Cl 99%; Fluka) in the primary source. The mixture of helium carrier gas and (deuterated) chlorobenzene vapor was introduced into the piezoelectric pulsed valve (Proch-Trickl) operated at a rate of 120 Hz and a backing pressure of about 1.5 atm. The (deuterated) chlorobenzene was photolyzed by focusing the 193 nm excimer laser output operating at 60 Hz and with a peak power of 10 mJ per pulse 1 mm downstream of the nozzle prior to the skimmer. Under our experimental conditions, the photolysis of chlorobenzene was 90%, using 1 × 3 mm focal region, with an absorption cross section of 9.6 × 10⁻¹⁸ cm² at 193 nm.^[53] The molecular beam entraining the (deuterated) phenyl radical passed a skimmer and a four-slot chopper wheel, which selected a segment of the pulsed (deuterated) phenyl radical (C₆D₅, X²A₁) beam of a well-defined peak velocity (v_p) and speed ratio (S ; see Table 2 in the Supporting Information). The radical beam bisected a pulsed molecular beam of the neat hydrocarbon generated in the secondary source with a pulsed valve at a backing pressure of 550 torr fired 20 μs prior to the pulsed valve in the primary source (Table S2 in the Supporting Information). We would like to stress that the phenyl and vinylacetylene reactants were formed in supersonic expansions, and hence, had little internal energy. Based on previous investigations of photolytically generated methylidyne radicals,^[51] laser-induced fluorescence (LIF) studies suggested a rotational temperature of about 15 K. Unfortunately, currently no LIF scheme exists for the phenyl radical. The reaction products were monitored by using a triply differentially pumped quadrupole mass spectrometer (QMS) in the TOF mode after electron-impact ionization of the neutral molecules at 80 eV with an emission current of 2 mA. These charged particles were separated according to their mass-to-charge ratio by an Extrel QC 150 quadrupole mass spectrometer operated with an oscillator at 1.2 MHz; only ions with the desired m/z value passed through and were accelerated toward a stainless steel 'door knob' target coated with an aluminum layer and operated at a voltage of -22.5 kV. The ions hit the surface and initiated an electron cascade that was accelerated by the potential until they reached an aluminum-coated organic scintillator, the photon cascade of which was detected by a photomultiplier tube (PMT; Burle, Model 8850, oper-

ated at -1.35 kV). The signal from the PMT was then filtered by a discriminator (Advanced Research Instruments, Model F-100TD, level: 1.6 mV) prior to feeding into a Stanford Research System SR430 multi-channel scaler to record TOF spectra.^[54,55] TOF spectra were recorded at 2.5° intervals over the angular distribution with 2.6×10^5 TOF spectra recorded at each angle. The TOF spectra recorded at each angle and the product angular distribution in the laboratory frame (LAB) were fit with Legendre polynomials by using a forward-convolution routine.^[56,57] This method uses an initial choice of $P(E_T)$ and $T(\theta)$ in the center-of-mass reference frame (C.M.) to reproduce TOF spectra and a product angular distribution. It should be noted that a threshold energy for the reaction, E_0 , was included in the fit based on previous experiments and kinetic studies on this system.^[43,45,46] An energy-dependent cross section, $\sigma(E_c) \approx [1 - E_0/E_c]$, through the line-of-center model with the collision energy E_c for $E_c \geq E_0$ was incorporated into the fitting routine; note that the fits were relatively insensitive to variations in E_0 between 0 and 20 kJ mol $^{-1}$. The TOF spectra and product angular distribution obtained from the fit were then compared with the experimental data. The parameters $P(E_T)$ and $T(\theta)$ were iteratively optimized until the best fit was reached. The product flux contour map, $I(\theta, u) = P(u) \times T(\theta)$, reports the intensity of the reactively scattered products (I) as a function of the C.M. scattering angle (θ) and product velocity (u). This plot is called the reactive differential cross section and gives an image of the chemical reaction.

Theoretically, we utilized optimized geometries and vibrational frequencies of various species on the $C_6H_5 + C_3H_4$ potential energy surface from previous works^[46,47,48] calculated at the B3LYP-DFT/6-311+G** level of theory. Chemically accurate single-point energies were computed by using the G3(MP2,CC)/B3LYP modification^[58,59] of the original Gaussian 3 (G3) model chemistry scheme.^[60] The final energies at 0 K were thus obtained by using the B3LYP-optimized geometries and ZPE corrections according to Equation (1):

$$E_0[G3(MP2,CC)] = E[CCSD(T)/6-311G(d,p)] + \Delta E_{MP2} + E(ZPE) \quad (1)$$

in which $\Delta E_{MP2} = E[MP2/G3Large] - E[MP2/6-311G(d,p)]$ is the basis set correction and $E(ZPE)$ is the ZPE. $\Delta E(SO)$, a spin-orbit correction, and $\Delta E(HLC)$, a higher level correction, from the original G3 scheme were not included in our calculations because they do not make significant contributions to the relative energies. We used the Gaussian 98^[61] program package to carry out MP2 calculations, and the Molpro 2002^[62] program package to perform calculations of spin-restricted coupled cluster RCCSD(T) energies. With the energetic and molecular parameters in hand, we employed RRKM theory^[63-65] for computations of rate constants of individual unimolecular reaction steps on the C_6H_5 PES. Rate constants, $k(E)$, were calculated as functions of the internal energy, which was taken as a sum of the energy of chemical activation in the phenyl plus allene/methylacetylene reactions and a collision energy, assuming that a dominant fraction of the latter is converted to the internal vibrational energy. The harmonic approximation was used to calculate the total number and density of states. Product branching ratios were computed by solving first-order kinetic equations for unimolecular reactions according to the kinetics scheme devised from the ab initio potential energy diagram shown in Figure 6, in which Rad 1 (methylacetylene) and Rad 11 or Rad 6 (allene) were considered as the initial chemically activated reaction intermediates. Only a single total-energy level was considered throughout; single-collision conditions (zero-pressure limit) and the steady-state approximation were used to obtain the branching ratios.^[66]

Acknowledgements

This work was supported by grants from the US Department of Energy, Basic Energy Sciences (DE-FG02-03ER15411 to the University of Hawaii and DE-FG02-04ER15570 to Florida International University).

[1] W. M. Baird, L. A. Hooven, B. Mahadevan, *Environ. Mol. Mutagen.* **2005**, *45*, 106.

- [2] M. F. Denissenko, A. Pao, M.-s. Tang, G. P. Pfeifer, *Science* **1996**, *274*, 430.
- [3] B. J. Finlayson-Pitts, J. N. Pitts, Jr., *Science* **1997**, *276*, 1045.
- [4] B. M. Jones, F. Zhang, R. I. Kaiser, A. Jamal, A. M. Mebel, M. A. Cordiner, S. B. Charnley, *Proc. Natl. Acad. Sci. USA* **2011**, *108*, 452.
- [5] C. Huang, F. Zhang, R. I. Kaiser, V. V. Kislov, A. M. Mebel, R. Silva, W. K. Gichuhi, A. G. Suits, *Astrophys. J.* **2010**, *714*, 1249.
- [6] M. Frenklach, *Phys. Chem. Chem. Phys.* **2002**, *4*, 2028.
- [7] M. Frenklach, T. Yuan, M. K. Ramachandra, *Energy Fuels* **1988**, *2*, 462.
- [8] D. K. Hahn, S. J. Klippenstein, J. A. Miller, *Faraday Discuss.* **2001**, *119*, 79.
- [9] H. Richter, J. B. Howard, *Phys. Chem. Chem. Phys.* **2002**, *4*, 2038.
- [10] J. A. Miller, M. J. Pilling, J. Troe, *Proc. Combust. Inst.* **2005**, *30*, 43.
- [11] N. Hansen, T. Kasper, S. J. Klippenstein, P. R. Westmoreland, M. E. Law, C. A. Taatjes, K. Kohse-Hoinghaus, J. Wang, T. A. Cool, *J. Phys. Chem. A* **2007**, *111*, 4081.
- [12] L. B. Harding, S. J. Klippenstein, Y. Georgievskii, *J. Phys. Chem. A* **2007**, *111*, 3789.
- [13] J. A. Miller, *Symp. (Int.) Combust. [Proc.]* **1996**, *26*, 461.
- [14] R. D. Kern, K. Xie, *Prog. Energy Combust.* **1991**, *17*, 191.
- [15] C. S. McEnally, L. D. Pfefferle, A. G. Robinson, T. S. Zwier, *Combust. Flame* **2000**, *123*, 344.
- [16] J. A. Miller, S. J. Klippenstein, *J. Phys. Chem. A* **2003**, *107*, 7783.
- [17] J. A. Miller, C. F. Melius, *Combust. Flame* **1992**, *91*, 21.
- [18] S. Scherer, T. Just, P. Frank, *Proc. Combust. Inst.* **2000**, *28*, 1511.
- [19] F. Zhang, B. Jones, P. Maksyutenko, R. I. Kaiser, C. Chin, V. V. Kislov, A. M. Mebel, *J. Am. Chem. Soc.* **2010**, *132*, 2672.
- [20] P. Dagaut, M. Cathonnet, *Combust. Flame* **1998**, *113*, 620.
- [21] R. I. Kaiser, O. Asvany, Y. T. Lee, H. F. Bettinger, P. v. R. Schleyer, H. F. Schaefer III, *J. Chem. Phys.* **2000**, *112*, 4994.
- [22] R. I. Kaiser, L. Vereecken, J. Peeters, H. F. Bettinger, P. v. R. Schleyer, H. F. Schaefer III, *Astron. Astrophys.* **2003**, *406*, 385.
- [23] T. R. Melton, F. Inal, S. M. Senkan, *Combust. Flame* **2000**, *121*, 671.
- [24] T. R. Melton, A. M. Vincitore, S. M. Senkan, *Symp. (Int.) Combust. [Proc.]* **1998**, *27*, 1631.
- [25] Y. Li, Z. Tian, L. Zhang, T. Yuan, K. Zhang, B. Yang, F. Qi, *Proc. Combust. Inst.* **2009**, *32*, 647.
- [26] Y. Li, L. Zhang, Z. Tian, T. Yuan, J. Wang, B. Yang, F. Qi, *Energy Fuels* **2009**, *23*, 1473.
- [27] Y. Li, L. Zhang, Z. Tian, T. Yuan, K. Zhang, B. Yang, F. Qi, *Proc. Combust. Inst.* **2009**, *32*, 1293.
- [28] Y. Li, L. Zhang, T. Yuan, K. Zhang, J. Yang, B. Yang, F. Qi, C. K. Law, *Combust. Flame* **2010**, *157*, 143.
- [29] M. Kamphus, M. Braun-Unkloff, K. Kohse-Hoinghaus, *Combust. Flame* **2008**, *152*, 28.
- [30] N. M. Marinov, W. J. Pitz, C. K. Westbrook, A. M. Vincitore, M. J. Castaldi, S. M. Senkan, C. F. Melius, *Combust. Flame* **1998**, *114*, 192.
- [31] J. J. Newby, J. A. Stearns, C.-P. Liu, T. S. Zwier, *J. Phys. Chem. A* **2007**, *111*, 10914.
- [32] B. Yang, Y. Li, L. Wei, C. Huang, J. Wang, Z. Tian, R. Yang, L. Sheng, Y. Zhang, F. Qi, *Proc. Combust. Inst.* **2007**, *31*, 555.
- [33] T. Zhang, L. Zhang, X. Hong, K. Zhang, F. Qi, C. K. Law, T. Ye, P. Zhao, Y. Chen, *Combust. Flame* **2009**, *156*, 2071.
- [34] D. H. Kim, J. A. Mulholland, D. Wang, A. Violi, *J. Phys. Chem. A* **2010**, *114*, 12411.
- [35] A. Lamprecht, B. Atakan, K. Kohse-Hoinghaus, *Proc. Combust. Inst.* **2000**, *28*, 1817.
- [36] M. Lu, J. A. Mulholland, *Chemosphere* **2001**, *42*, 625.
- [37] R. P. Lindstedt, K. A. Rizos, *Proc. Combust. Inst.* **2002**, *29*, 2291.
- [38] D. Wang, A. Violi, D. H. Kim, J. A. Mulholland, *J. Phys. Chem. A* **2006**, *110*, 4719.
- [39] P. Lindstedt, L. Maurice, M. Meyer, *Faraday Discuss.* **2001**, *119*, 409.
- [40] J. D. Bittner, Ph.D. Thesis, Massachusetts Institute of Technology (USA), **1981**.
- [41] J. Park, I. V. Tokmakov, M. C. Lin, *J. Phys. Chem. A* **2007**, *111*, 6881.
- [42] I. V. Tokmakov, J. Park, M. C. Lin, *ChemPhysChem* **2005**, *6*, 2075.
- [43] X. Gu, F. Zhang, Y. Guo, R. I. Kaiser, *J. Phys. Chem. A* **2007**, *111*, 11450.

- [44] X. Gu, R. I. Kaiser, *Acc. Chem. Res.* **2009**, *42*, 290.
- [45] L. Vereecken, H. F. Bettinger, J. Peeters, *Phys. Chem. Chem. Phys.* **2002**, *4*, 2019.
- [46] L. Vereecken, J. Peeters, *Phys. Chem. Chem. Phys.* **2003**, *5*, 2807.
- [47] L. Vereecken, J. Peeters, H. F. Bettinger, R. I. Kaiser, P. v. R. Schleyer, H. F. Schaefer III, *J. Am. Chem. Soc.* **2002**, *124*, 2781.
- [48] R. I. Kaiser, *Chem. Rev.* **2002**, *102*, 1309.
- [49] R. D. Levine, *Molecular Reaction Dynamics and Chemical Reactivity*, Oxford University Press, Oxford, **1987**.
- [50] W. B. Miller, S. A. Safron, D. R. Herschbach, *Discuss. Faraday Soc.* **1967**, *44*, 108.
- [51] P. Maksyutenko, F. Zhang, X. Gu, R. I. Kaiser, *Phys. Chem. Chem. Phys.* **2011**, *13*, 240.
- [52] X. Gu, Y. Guo, F. Zhang, A. M. Mebel, R. I. Kaiser, *Faraday Discuss.* **2006**, *133*, 245.
- [53] W. G. Mallard, P. J. Linstrom, Eds. NIST Chemistry WebBook, National Institute of Standards and Technology, Gaithersburg, MD, **2000**.
- [54] X. B. Gu, Y. Guo, E. Kawamura, R. I. Kaiser, *Rev. Sci. Instrum.* **2005**, *76*, 083115/1.
- [55] Y. Guo, X. Gu, E. Kawamura, R. I. Kaiser, *Rev. Sci. Instrum.* **2006**, *77*, 034701/1.
- [56] M. Vernon, Ph.D. Thesis, University of California, Berkley (USA), **1981**.
- [57] M. S. Weis, Ph.D. Thesis, University of California, Berkley (USA), **1986**.
- [58] A. G. Baboul, L. A. Curtiss, P. C. Redfern, K. Raghavachari, *J. Chem. Phys.* **1999**, *110*, 7650.
- [59] L. A. Curtiss, K. Raghavachari, P. C. Redfern, A. G. Baboul, J. A. Pople, *Chem. Phys. Lett.* **1999**, *314*, 101.
- [60] L. A. Curtiss, K. Raghavachari, P. C. Redfern, V. Rassolov, J. A. Pople, *J. Chem. Phys.* **1998**, *109*, 7764.
- [61] Gaussian 98 (Revision A.10), M. J. Frisch, G. W. Trucks, H. B. Schlegel, G. E. Scuseria, M. A. Robb, J. R. Cheeseman, V. G. Zakrzewski, J. A. Montgomery, Jr., R. E. Stratmann, J. C. Burant, S. Dapprich, J. M. Millam, A. D. Daniels, K. N. Kudin, M. C. Strain, O. Farkas, J. Tomasi, V. Barone, M. Cossi, R. Cammi, B. Mennucci, C. Pomelli, C. Adamo, S. Clifford, J. Ochterski, G. A. Petersson, P. Y. Ayala, Q. Cui, K. Morokuma, P. Salvador, J. J. Dannenberg, D. K. Malick, A. D. Rabuck, K. Raghavachari, J. B. Foresman, J. Cioslowski, J. V. Ortiz, A. G. Baboul, B. B. Stefanov, G. Liu, A. Liashenko, P. Piskorz, I. Komaromi, R. Gomperts, R. L. Martin, D. J. Fox, T. Keith, M. A. Al-Laham, C. Y. Peng, A. Nanayakkara, M. Challacombe, P. M. W. Gill, B. Johnson, W. Chen, M. W. Wong, J. L. Andres, C. Gonzalez, M. Head-Gordon, E. S. Replogle, J. A. Pople, Gaussian, Inc., Pittsburgh PA, **2001**.
- [62] MOLPRO: A package of ab initio programs, version 2002.1, R. D. Amos, A. Bernhardsson, A. Berning, P. Celani, D. L. Cooper, M. J. O. Deegan, A. J. Dobbyn, F. Eckert, C. Hampel, G. Hetzer, P. J. Knowles, T. Korona, R. Lindh, A. W. Lloyd, S. J. McNicholas, F. R. Manby, W. Meyer, M. E. Mura, A. Nicklass, P. Palmieri, R. Pitzer, G. Rauhut, M. Schutz, U. Schumann, H. Stoll, A. J. Stone, R. Tarroni, T. Thorsteinsson, H.-J. Werner, Cardiff University, Cardiff, UK, **2002**.
- [63] H. Eyring, S. H. Lin, S. M. Lin, *Basic Chemical Kinetics*, Wiley, New York, **1980**.
- [64] P. J. Robinson, K. A. Holbrook, *Unimolecular Reactions*, Wiley, New York, **1972**.
- [65] J. I. Steinfeld, J. S. Francisco, W. L. Hase, *Chemical Kinetics and Dynamics*, Prentice Hall, Engelwood Cliffs, NJ, **1999**.
- [66] V. V. Kislov, T. L. Nguyen, A. M. Mebel, S. H. Lin, S. C. Smith, *J. Chem. Phys.* **2004**, *120*, 7008.

Received: June 15, 2011
Published online: September 28, 2011